Comparative NMR investigation of the Re-based borides

C. S. Lue,* Y. F. Tao, and T. H. Su
Department of Physics, National Cheng Kung University, Tainan 70101, Taiwan
(Received 5 December 2007; published 11 July 2008)

We report a systematic study of the rhenium-based borides, ReB_2, Re_7B_3, and Re_3B, by means of the ^{11}B nuclear magnetic resonance (NMR) spectroscopy. While Re_7B_3 and Re_3B are superconductors, ReB_2 exhibits no superconducting signature but is of current interest due to its superhard mechanical property. Since the major focus of this investigation is their electronic characteristics in the normal states, we performed the measurements at temperatures between 77 and 295 K. For Re_7B_3 and Re_3B, *s*-character electrons were found to be responsible for the observed ^{11}B NMR Knight shift and spin-lattice relaxation rate $(1/T_1)$. From T_1 analysis, we thus deduce the partial B *s* Fermi-level density of states (DOS) of both borides. On the other hand, the relaxation rate of ReB_2 is mainly associated with *p* electrons, similar to the cases of OsB_2 and RuB_2. In addition, the extracted B 2*p* Fermi-level DOS is in good agreement with the theoretical prediction from band-structure calculations.

DOI: 10.1103/PhysRevB.78.033107 PACS number(s): 74.70.Ad, 74.25.Nf

I. INTRODUCTION

The discovery of superconductivity at the transition temperature $T_C=39$ K in MgB_2 has stimulated a large number of studies on the related metal borides.[1] Many investigations have been focused on the transition metal-based diborides with AlB_2-type crystal structure because of the two-dimensional honeycomb network between boron atoms, similar to MgB_2.[2] It is generally believed that the geometric arrangement of B atoms plays an important role for the superconductivity where the effect turns out to affect the electronic band features.[3] In addition to the AlB_2-type phase, the configuration of B atoms in other superconducting borides have been carefully examined.[4] Recently, a comparative study of physical properties in the normal and superconducting states of Re_7B_3 and Re_3B was reported by Kawano *et al.*[5] Both compounds crystallize in different structures with space groups of $P6_3/mc$ for Re_7B_3 and *Cmcm* for Re_3B, as shown in Fig. 1. Results indicated that the physical properties are relevant to the geometric arrangement of B atoms but no further specific information, essential to interpret the relationship between the crystal structure and electronic properties, was obtained in that study.

Nuclear magnetic resonance (NMR) measurement is known as an atomic probe in metallic alloys yielding information on the Fermi-surface features.[6] In this work, we present a systematic investigation of three rhenium borides ReB_2, Re_7B_3, and Re_3B by means of ^{11}B NMR measurements between 77 and 295 K. For comparison, we included the nonsuperconducting ReB_2 (space group $P6_3/mmc$) which has the highest B:Re ratio among the binary Re-based borides. This material has been reported to be a superhard material[7] and the strong covalent bonding of B-B and Re-B has been proposed to be the key source responsible for the unusual mechanical property.[8–12] Hence the present NMR study of the electronic characteristics would provide an experimental insight for the comparison to theoretical predictions.

II. EXPERIMENT

Polycrystalline samples were prepared from 99.99% Re and 99.9% B by mixing appropriate amounts of elemental metals, pressing the mixtures into small pellets, and melting them in an Ar arc furnace. Each material was melted several times, and the weight loss during melting is less than 1%. To promote homogeneity, these compounds were annealed in a vacuum-sealed quartz tube at 900 °C for seven days and followed by furnace cooling.

Magnetic susceptibility was measured using a superconducting quantum interference device magnetometer (Quantum Design Co. Ltd.). NMR experiments were performed using a Varian 300 spectrometer, with a constant field of 6.944 T. A home-built probe was employed for both room-temperature and low-temperature experiments.[13] Since the studied materials are metals, powder samples were used to avoid the skin depth problem of the rf transmission power. Each specimen was put in a plastic vial that showed no observable ^{11}B NMR signal.

III. RESULTS AND DISCUSSION

In Fig. 2, we show the temperature dependence of magnetic susceptibility measured at 10 Oe under a zero-field-cooled condition. For Re_7B_3 and Re_3B, they clearly exhibit diamagnetic drops below the transition temperatures of approximately 3.1 and 4.6 K, respectively. The observed T_Cs are quite close to the values reported by Kawano *et al.*,[5] indicating a similar sample quality. Also the absence of su-

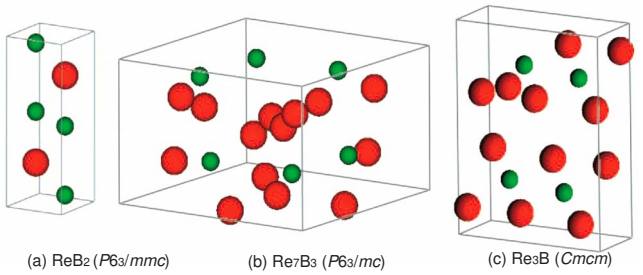

FIG. 1. (Color online) Crystal structures for ReB_2, Re_7B_3, and Re_3B. The large red and small green balls represent the Re and B atoms, respectively.

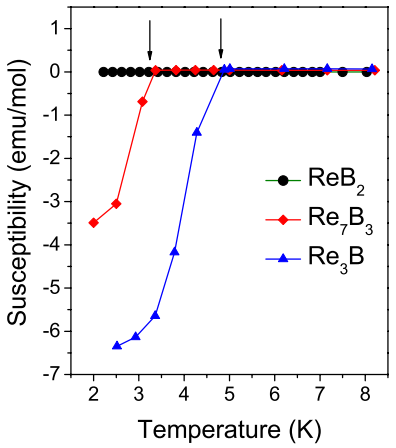

FIG. 2. (Color online) Temperature dependence of magnetic susceptibility measured at 10 Oe under a zero-field-cooled condition. The arrows indicate the superconducting transition temperatures for Re_7B_3 and Re_3B.

perconducting behavior in ReB_2 is consistent with the recent observation although an early study of this material indicated superconducting transitions from 4.5 to 6.3 K.[14] The discrepancy has been speculated to be due to nonstoichiometric effects.

NMR central transition lines of the studied compounds were obtained from the Fourier transform of the solid echo pulse sequence at 295 K and spin-echo integral of various excitations at 77 K. For each individual crystal structure, there is a single B site, leading to a one-site NMR powder pattern, as displayed in Fig. 3. There are no detectable change in the NMR spectra and frequency shifts in the normal state, consistent with the typical feature for nonmagnetic metals. While ^{11}B NMR resonance is dipolar broadened ($I=\frac{3}{2}$), we found no visible satellite lines in a wide frequency range. This could be attributed to the nonaxial symmetry for the B crystallographic site. Within these structures, the corresponding asymmetry parameter $\eta \equiv |V_{xx}-V_{yy}|/|V_{zz}|$ is expected to be large. Such an asymmetric effect will smear out the edge of the satellite lines, resulting in the unresolved transition lines in these compounds.

The ^{11}B isotropic Knight shift (K) here was determined from the position of the maximum of each spectrum with respect to an aqueous $NaBH_4$ solution reference. As shown in the inset of Fig. 3, the Knight shifts of these borides are temperature independent, a typical response for ordinary metals. For ReB_2, an extremely small Knight shift of about 10 ppm was found, similar to other transition metal borides[15] as well as MgB_2 (Refs. 13, 16, and 17). Such a tiny shift could be attributed to few s-character electrons at the Fermi surfaces. In fact, recent theoretical calculations on ReB_2 indicated that B $2p$ bands are all at the Fermi level with very few s-boron electrons near the Fermi surfaces.[8–12] Also the p electrons have little contribution to the Knight shift because of a low hyperfine field from p states. This argument is valid for MgB_2 in spite of its high B $2p$ Fermi-level density of states (DOS). On the contrary, relative large Knight shifts appear in Re_7B_3 and Re_3B, which is not likely due to p electrons. Instead, s-character electrons could be responsible for the observed shifts in both materials.

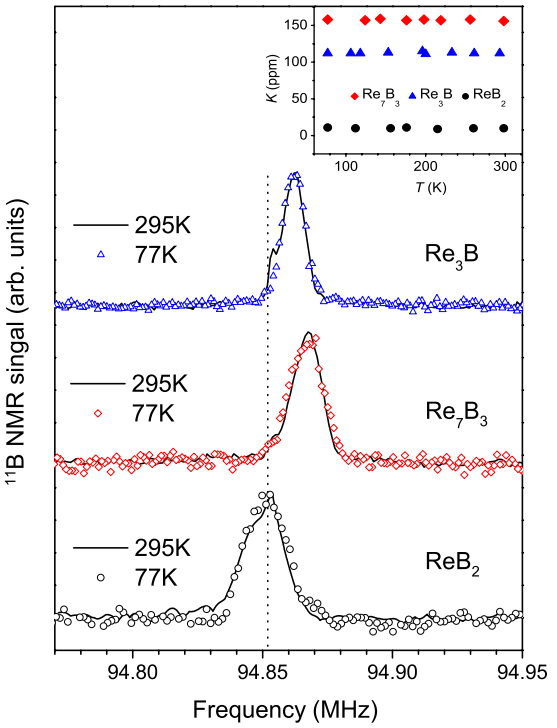

FIG. 3. (Color online) ^{11}B NMR central transition line shapes for ReB_2, Re_7B_3, and Re_3B measured at 295 and 77 K. The dotted line indicates the frequency for the zero ^{11}B Knight shift. The inset shows the temperature-independent Knight shifts for these borides.

The spin-lattice relaxation time (T_1) measurements were carried out by centering the resonance frequency at $m=-\frac{1}{2} \leftrightarrow +\frac{1}{2}$ transition line using the inversion recovery method. We recorded the signal strength by integrating the recovered spin-echo signal. In these experiments, the relaxation process involves the adjacent pairs of spin levels, and the corresponding relaxation is a multiexponential expression. For the central transition with $I=\frac{3}{2}$, the recovery of the nuclear magnetization follows:

$$\frac{M(t)-M(\infty)}{M(\infty)} = -2\alpha\left(\frac{1}{10}e^{-t/T_1}+\frac{9}{10}e^{-6t/T_1}\right). \quad (1)$$

Here $M(t)$ is the magnetization at the recovery time t and $M(\infty)$ is the magnetization after long time recovery. The parameter α is a fractional value derived from the initial conditions used in our experiments. Our T_1 values were thus obtained by fitting to this multiexponential recovery curve. While nonconduction mechanisms may contribute to the relaxation, they were excluded by the Korringa relation (constant T_1T).[18] In Fig. 4, the plot of $1/T_1$ vs T demonstrates the Korringa behavior shown as solid lines, indicative of a conduction-electron mechanism for the observed relaxation. The determined T_1Ts are also enumerated in Table I.

In paramagnetic metals, the spin-lattice relaxation rate measurement is a direct probe of the features of the Fermi surfaces.[19] While the relaxation of nuclei in a metal is normally governed by their coupling to the spin of s-character electrons, other mechanisms such as orbital and dipolar relaxations from p states become important when the Fermi-

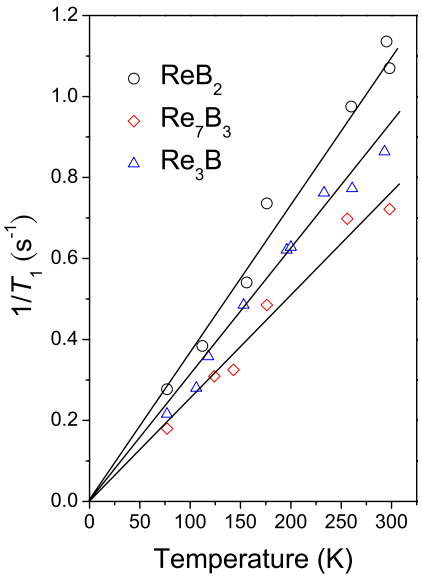

FIG. 4. (Color online) Temperature dependent ^{11}B spin-lattice relaxation rates of ReB_2, Re_7B_3, and Re_3B. Solid lines indicate the Korringa behavior.

contact term is essentially small.[20] This is true for ReB_2. As revealed from band-structure calculations,[8–10,12] only few *s*-boron electrons appear in the vicinity of the Fermi level of ReB_2. The low *s*-character Fermi-level DOS $N_s(E_F)$ should have a minor contribution to the total relaxation rate, in spite of a stronger hyperfine field arising from *s* electrons. A convincing result can be established from the Korringa ratio $R \equiv K^2 T_1 T / S \simeq 0.01$ for ReB_2. Here $S \equiv K_s^2 (T_1 T)_s = 2.57 \times 10^{-6}$ sec K for ^{11}B is derived from the contact interaction with *s* electrons for both *K* and T_1. Apparently, the ratio much less than unity indicates that T_1 could be driven by other relaxation mechanisms different from *s*-character electrons. This gives the dominant *p* orbital and dipolar relaxation rates as $(1/T_1)_p = (1/T_1)_{\mathrm{orb}} + (1/T_1)_{\mathrm{dip}}$.. It is worthwhile mentioning that a recent ^{11}B NMR study of OsB_2 and RuB_2 also showed the *p* electrons responsible for the observed relaxation rates.[21]

For the isotropic *p* orbitals, the experimental $1/T_1T$ can be simply expressed as

$$(T_1T)_p^{-1} = \frac{13}{45} C [H_{hf}^{\mathrm{orb}} N_p(E_F)]^2, \tag{2}$$

with $C = 2hk_B\gamma_n^2$. Here *h*, k_B, and γ_n are the Planck constant, the Boltzmann constant, and the nuclear gyromagnetic ratio, respectively. $N_p(E_F)$ is the partial B 2*p* Fermi-level DOS in units of states/eV spin. H_{hf}^{orb} represents the orbital hyperfine field per unit orbital angular momentum and can be evaluated using $H_{hf}^{\mathrm{orb}} = 2\mu_B \langle r^{-3} \rangle_p$, where $\langle r^{-3} \rangle_p$ is the average over the occupied *p* orbitals. Taking an estimated value of $1.65a_B$ for the boron radius of *p* electrons in ReB_2,[15] it yields $\langle r^{-3} \rangle_p = 1.35 \times 10^{25}$ cm^{-3}, corresponding to $H_{hf}^{\mathrm{orb}} = 2.5 \times 10^5$ G. With the above relationship and experimental NMR T_1T, we can thus extract $N_p(E_F) = 0.24$ states/eV f.u.. This result is in good agreement with 0.2–0.3 states/eV obtained from band-structure calculations,[10,11] suggesting a reliable estimate for the present analysis. It is interesting that the deduced $N_p(E_F)$ in ReB_2 is approximately two times larger than in OsB_2 and RuB_2.[21,22] In general, a higher Fermi-level DOS will reflect itself to a larger bulk modulus and hence higher incompressibility. With this accordance, our NMR study implies that ReB_2 possesses a higher bulk modulus than OsB_2 and RuB_2, being consistent with other experimental results.[7,23,24]

On the other hand, the above analysis would not be appropriate for Re_7B_3 and Re_3B. As in the case of the Knight shift, the Fermi-contact mechanism would dominate the observed ^{11}B relaxation rates. This argument is confirmed from $R \simeq 4$ for Re_7B_3 and $R \simeq 1.5$ for Re_3B. The Korringa ratio greater than unity is a common observation in ordinary metals, presumably due to additional contribution from the orbital shift and a slightly enhancement from electronic correlations. With this respect, the *s*-character electrons would be the major origin responsible for the relaxation rates in Re_7B_3 and Re_3B, and the corresponding $1/T_1T$ can be written as[25]

$$(T_1T)_s^{-1} = C [H_{hf}^s N_s(E_F)]^2, \tag{3}$$

where H_{hf}^s is the hyperfine field per electron and $N_s(E_F)$ represents the partial *s* DOS at the Fermi level. Taking $H_{hf}^s \sim 1 \times 10^6$ G in B metals[20] and experimental T_1Ts, each individual $N_s(E_F)$ can be obtained from Eq. (3). As one can see from Table I, the extracted $N_s(E_F)$ values are small in Re_7B_3 and Re_3B. However, we consider that $N_s(E_F)$ is not neglecting small as compared to $N_p(E_F)$ for both materials. This can be simply interpreted as the less hybridization between Re 5*d* and B 2*p* electrons in Re_7B_3 and Re_3B. According to their crystal structures, the covalent bonding in Re_7B_3 and Re_3B is not expected to be as strong as in ReB_2. As a consequence, the B Fermi-level DOS is not predominated by *p* bands. To further verify this point, other experimental and theoretical DOS data of Re_7B_3 and Re_3B are highly desirable.

TABLE I. Transition temperature, Knight shift, T_1T, partial B *s*, and 2*p* Fermi-level DOS in units of states/eV f.u. for each studied boride.

Alloy	T_C (K)	*K* (ppm)	T_1T (sK)	$N_s(E_F)$	$N_p(E_F)$
ReB_2		$\simeq 10$	280 ± 30		0.24
Re_7B_3	3.1 ± 0.2	$\simeq 160$	400 ± 40	0.041	
Re_3B	4.6 ± 0.3	$\simeq 110$	320 ± 30	0.015	

IV. CONCLUSIONS

We have a concise picture of the NMR features for ReB_2, Re_7B_3, as well as Re_3B, giving an experimental viewpoint for their local electronic properties. Analyses of the Knight shift and spin-lattice relaxation rate indicate that *p* states are dominant for the B crystallographic site of ReB_2 around the Fermi surfaces. Agreement is obtained for the deduced B 2*p* Fermi-level DOS as compared to theoretical results. On the

other hand, the Knight shifts and relaxation rates of Re_7B_3 and Re_3B are mainly associated with *s*-character electrons. We also extracted the *s*-component Fermi-level DOS for both compounds and called for other experimental and theoretical results for comparison.

ACKNOWLEDGMENTS

We were grateful for the support from the National Science Council of Taiwan under Grant No. NSC-95-2112-M-006-021-MY3 (C.S.L).

*cslue@mail.ncku.edu.tw

[1] J. Nagamatsu, N. Nakagawa, T. Muranaka, Y. Zenitani, and J. Akimitsu, Nature (London) **410**, 63 (2001).
[2] A. L. Ivanovskii, Phys. Solid State **45**, 1829 (2003), and references therein.
[3] Tamio Oguchi, J. Phys. Soc. Jpn. **71**, 1495 (2002).
[4] P. Ravindran, P. Vajeeston, R. Vidya, A. Kjekshus, and H. Fjellvag, Phys. Rev. B **64**, 224509 (2001).
[5] Akihiko Kawano, Yukiko Mizuta, Hiroyuki Takagiwa, Takahiro Muranaka, and Jun Akimitsu, J. Phys. Soc. Jpn. **72**, 1724 (2003).
[6] C. S. Lue, T. H. Su, B. X. Xie, and C. Cheng, Phys. Rev. B **74**, 094101 (2006).
[7] H.-Y. Chung, M. B. Weinberger, J. B. Levine, A. Kavner, J.-M. Yang, S. H. Tolbert, and R. B. Kaner, Science **316**, 436 (2007).
[8] Xianfeng Hao, Yuanhui Xu, Zhijian Wu, Defeng Zhou, Xiaojuan Liu, Xueqiang Cao, and Jian Meng, Phys. Rev. B **74**, 224112 (2006).
[9] Yongcheng Liang and Bin Zhang, Phys. Rev. B **76**, 132101 (2007).
[10] W. Zhou, H. Wu, and T. Yildirim, Phys. Rev. B **76**, 184113 (2007).
[11] Yuan Xu. Wang, Appl. Phys. Lett. **91**, 101904 (2007).
[12] R. F. Zhang, S. Veprek, and A. S. Argon, Appl. Phys. Lett. **91**, 201914 (2007).
[13] C. S. Lue, T. H. Su, B. X. Xie, S. K. Chen, J. L. MacManus-Driscoll, Y. K. Kuo, and H. D. Yang, Phys. Rev. B **73**, 214505 (2006).
[14] G. K. Strukova, V. F. Degtyareva, D. V. Shovkun, V. N. Zverev, V. M. Kiiko, A. M. Ionov, and A. N. Chaika, arXiv:cond-mat/0105293 (unpublished).
[15] C. S. Lue and W. J. Lai, Phys. Status Solidi B **242**, 1108 (2005).
[16] S. Serventi, G. Allodi, C. Bucci, R. De Renzi, G. Guidi, E. Pavarini, P. Manfrinetti, and A. Palenzona, Phys. Rev. B **67**, 134518 (2003).
[17] S. H. Baek, B. J. Suh, E. Pavarini, F. Borsa, R. G. Barnes, S. L. Bud'ko, and P. C. Canfield, Phys. Rev. B **66**, 104510 (2002).
[18] J. Korringa, Physica (Amsterdam) **16**, 601 (1950).
[19] C. P. Slichter, *Principles of Magnetic Resonance* (Springer-Verlag, New York, 1990).
[20] *Metallic Shifts in NMR*, edited by G. C. Carter, L. H. Bennett, and D. J. Kahan (Pergamon, Oxford, 1977).
[21] B. J. Suh, X. Zong, Y. Singh, A. Niazi, and D. C. Johnston, Phys. Rev. B **76**, 144511 (2007).
[22] S. Chiodo, H. J. Gotsis, N. Russo, and E. Sicilia, Chem. Phys. Lett. **425**, 311 (2006).
[23] R. B. Kaner, J. J. Gilman, and S. H. Tolbert, Science **308**, 1268 (2005).
[24] R. W. Cumberland, M. B. Weinberger, J. J. Gilman, S. M. Clark, S. H. Tolbert, and R. B. Kaner, J. Am. Chem. Soc. **127**, 7264 (2005).
[25] A. Abragam, *Principles of Nuclear Magnetism* (Oxford University Press, New York, 1982).